Original Paper

Cellular Physiology and Biochemistry

In vitro Modeling of Ryanodine Receptor 2 Dysfunction Using Human Induced Pluripotent Stem Cells

Azra Fatima[1], Guoxing Xu[1], Kaifeng Shao[1], Symeon Papadopoulos[2], Martin Lehmann[1], Juan J. Arnáiz-Cot[3], Angelo O. Rosa[3], Filomain Nguemo[1], Matthias Matzkies[1], Sven Dittmann[4], Susannah L. Stone[3], Matthias Linke[5], Ulrich Zechner[5], Vera Beyer[5], Hans Christian Hennies[6,8,9], Stephan Rosenkranz[7,8], Baerbel Klauke[4], Abdul S. Parwani[10], Wilhelm Haverkamp[10], Gabriele Pfitzer[2], Martin Farr[4], Lars Cleemann[3], Martin Morad[3], Hendrik Milting[4], Juergen Hescheler[1] and Tomo Šarić[1]

[1]Institute for Neurophysiology and [2]Vegetative Physiology, Medical Center, University of Cologne, Cologne, [3]Cardiac Signaling Center, Medical University of South Carolina, Charleston, [4]Heart and Diabetes Center NRW, University Hospital of the Ruhr-University of Bochum, Erich and Hanna Klessmann-Institute for Cardiovascular Research and Development, Bochum, [5]Institute for Human Genetics, Johannes Gutenberg University, Mainz, [6]Cologne Center for Genomics, University of Cologne, Cologne, [7]Clinic III for Internal Medicine, Heart Center, University of Cologne, Cologne, [8]Center for Molecular Medicine Cologne, University of Cologne, Cologne, [9]Cluster of Excellence on Cellular Stress Responses in Aging-associated Diseases, University of Cologne, Cologne, [10]Charité-Universitaetsmedizin, Medical Department, Division of Cardiology, Campus Virchow Klinikum, Berlin

Abstract
Background/Aims: Induced pluripotent stem (iPS) cells generated from accessible adult cells of patients with genetic diseases open unprecedented opportunities for exploring the pathophysiology of human diseases *in vitro*. Catecholaminergic polymorphic ventricular tachycardia type 1 (CPVT1) is an inherited cardiac disorder that is caused by mutations in the cardiac ryanodine receptor type 2 gene (*RYR2*) and is characterized by stress-induced ventricular arrhythmia that can lead to sudden cardiac death in young individuals. The aim of this study was to generate iPS cells from a patient with CPVT1 and determine whether iPS cell-derived cardiomyocytes carrying patient specific *RYR2* mutation recapitulate the disease phenotype *in vitro*. Methods: iPS cells were derived from dermal fibroblasts of healthy donors and a patient with CPVT1 carrying the novel heterozygous autosomal dominant mutation p.F2483I in the *RYR2*. Functional properties of iPS cell derived-cardiomyocytes were analyzed by using whole-cell current and voltage clamp and calcium imaging techniques. Results: Patch-clamp recordings revealed arrhythmias and delayed afterdepolarizations (DADs) after catecholaminergic stimulation of CPVT1-iPS cell-

Tomo Šarić, M.D., Ph.D.
Center for Physiology and Pathophysiology, Unikliniken Koeln
University of Cologne, Robert Koch Str. 39, 50931 Cologne (Germany)
Tel. +49-221-478-86686, Fax +49-221-478-3834
E-Mail tomo.saric@uni-koeln.de

derived cardiomyocytes. Calcium imaging studies showed that, compared to healthy cardiomyocytes, CPVT1-cardiomyocytes exhibit higher amplitudes and longer durations of spontaneous Ca^{2+} release events at basal state. In addition, in CPVT1-cardiomyocytes the Ca^{2+}-induced Ca^{2+}-release events continued after repolarization and were abolished by increasing the cytosolic cAMP levels with forskolin. Conclusion: This study demonstrates the suitability of iPS cells in modeling RYR2-related cardiac disorders *in vitro* and opens new opportunities for investigating the disease mechanism *in vitro*, developing new drugs, predicting their toxicity, and optimizing current treatment strategies.

Introduction

In vitro culture of cardiomyocytes isolated from patients with arrhythmias or other inherited heart diseases may advance our understanding of disease mechanisms at the molecular and cellular level and enable development of new therapeutic strategies. However, cardiomyocytes that can be obtained from patient biopsies have a disadvantage of not being easily accessible at sufficient quantities and of having only a short survival time *in vitro*. Induced pluripotent stem (iPS) cells [1] represent an alternative, easily accessible and expandable source of disease specific cell types, and thus offer an unprecedented opportunity to investigate the molecular mechanisms of disease *in vitro*, and develop new drugs or test their toxicity [2, 3].

It is now firmly established that human iPSC-derived cardiomyocytes have similar molecular and functional properties to those of their embryonic stem cell (ES) cell-derived counterparts, suggesting that they may represent a suitable *in vitro* experimental model [4-10]. In addition to human *in vitro* iPS cell-based disease models for a large number of non-cardiac diseases [11-23], iPS cell models have been also established for congenital diseases affecting the heart. So far, the heart disease specific iPS cells have been reported for the LEOPARD syndrome [24] and the three long-QT syndromes LQTS1 [25], LQTS2 [26, 27] and Tymothy syndrome [28]. These studies have demonstrated that cardiomyocytes differentiated from these iPS cells exhibit the cardiac electrical disturbances characteristic of each particular disease. Moreover, the disease phenotype in LQTS-

cardiomyocytes could be reversed by specific drugs, confirming the potential of these models for use in drug development.

Catecholaminergic polymorphic ventricular tachycardia (CPVT) is an inherited cardiac disorder characterized by emotional and physical stress-induced ventricular tachyarrhythmia, syncope and sudden cardiac death in children and young adults [29]. CPVT affects about one in 10,000 people and it is estimated to cause 15% of all unexplained sudden cardiac deaths in young people [30]. In 30-40% of cases, the autosomal dominant form of CPVT (type 1) has been linked to mutations in the cardiac ryanodine receptor type 2 gene (*RYR2*) encoding a Ca^{2+} channel in the membrane of the sarcoplasmic reticulum (SR). However, a rare autosomal recessive form of CPVT (type 2) is caused by mutations in the calsequestrin-2 gene [31]. To date, more than 150 mutations have been identified in the *RYR2* gene in CPVT1 (MIM 604772; http://www.fsm.it/cardmoc/) [32]. Studies based on *in vitro* expression of mutant RYR2 in heterologous cell systems [33] and transgenic mice carrying specific *RYR2* mutations [34] suggested that arrhythmias in CPVT1 are precipitated by the diastolic Ca^{2+} leak from the SR triggering delayed afterdepolarizations (DADs) following catecholaminergic stimulation [35, 36]. However, the exact mechanism leading to this defect is not completely understood and models for investigating the pathogenesis of this disease and developing better treatment strategies using easily accessible human patient-specific cardiomyocytes are still missing. In this study we have generated iPS cell lines from a patient with CPVT1 carrying the novel mutation p.F2483I in the *RYR2* gene and show that cardiomyocytes derived from mutant cells recapitulate the disease phenotype *in vitro*, thus offering a new tool for studying the molecular basis of this disease and improving its pharmacotherapy.

Materials and Methods

Reprogramming and cell culture
The collection of skin biopsies from the patient and healthy volunteers was approved by the Ethics Committee of the Medical Faculty of the University of Cologne (permit No. 08-262) and was carried out after informed consent. Biopsy specimens were cut into small pieces and placed on culture dishes to allow for fibroblast expansion. At third passage, 20,000 cells were infected with equal amounts of pMXs-based retroviruses (Addgene) encoding the human genes OCT3/4, SOX2, KLF4, and c-MYC as described previously [1, 37]. Cells were transduced in the presence of 4 μg/ml polybrene (Sigma)

Fatima/Xu/Shao/Papadopoulos/Lehmann/Arnáiz-Cot/Rosa/Nguemo/
Matzkies/Dittmann/Stone/Linke/Zechner/Beyer/Hennies/Rosenkranz/
Klauke/Parwani/Haverkamp/Pfitzer/Farr/Cleemann/Morad/Milting/
Hescheler/Šarić

Gene	Sequence (5' to 3')	NCBI Accession #	Amplicon size (nt)	Annealing temp., °C
OCT4	F: AGGGCAAGCGATCAAGCA R: GGAAAGGGACCGAGGAGTA	NM_002701	168	60
NANOG	F: ACTAACATGAGTGTGGATCC R: TCATCTTCACACGTCTTCAG	NM_024865.2	130	60
SOX2	F: ATGCACCGCTACGACGTGA R: CTTTTGCACCCCTCCCATTT	NM_003106.2	437	60
REX1	F:GACAGAGGTCACGCAAGAGA R:TTGAAATCCAGGGAGAAACG	NM_009556	333	60
KLF4rv	F: CCACCTCGCCTTACACATGA R: CCCTTTTTCTGGAGACTAAATAAA	NM_004235.4	150	60
cMYCrv	F:GGAAACGACGAGAACAGTTGA R: CCCTTTTTCTGGAGACTAAATAAA	NM_002467.4	300	60
OCT4rv	F: GCTCTCCCATGCATTCAAAC R: TTATCGTCGACCACTGTGCTGCTG	NM_001159542.1	200	60
SOX2rv	F: GGCCATTAACGGCACACTG R: CCCTTTTTCTGGAGACTAAATAAA	NM_003106.2	250	60
RyR2	F: CTGGTGAGGAAGAAGCCAAG R: TGTCTTCCTGGCTGTGAGTG	NM_001035.2	204	60
RyR2seq	F: GTAAGAAGTCTAGAAAGCAGC R: CCTGAAAATATAACAGGTACTC	NM_001035.2	383	61
MYH6	CCGATACTGGGGACAGT GGT CGTAGAGGATGCGGTTGG	NM_002471.3	270	60
MYL2	F: ACAGGGATGGCTTCATTGAC R: CCTCCTCCTTGGAAAACCTC	NM_000432.3	288	60
ACTN2	F: GGCACCCAGATTGAGAACAT R: CCTGAATAGCAAAGCGAAGG	NM_001103.1	268	60
SERCA	F:CTGTGTGGCTGTCTGGCTTA R:CAGACATCTGGTTGGTGGTG	NM_173201.3		60

Table 1. List of primer sequences used for PCR analyses. *rv* - primers used for amplification of retroviral sequences; *seq* - primers used for sequencing.

for 8 h per day for 2 days and maintained in high glucose DMEM, 10% fetal bovine serum (FBS), 1% nonessential amino acids (NAA), 1x penicillin/streptomycin, L-glutamine, 0.1 mmol/L β-mercaptoethanol (βME) and 50 ng/ml bFGF (Peprotech), (DFBS medium). Six days after the first infection, 10,000 cells were plated on gelatin-coated 60 mm dishes containing 5×10^5 irradiated CF1 MEFs. From day 7, plates were maintained in DFBS-containing medium supplemented with 20 μg/ml vitamin C and 1 mM valproic acid (Sigma). ESC-like colonies appeared between day 21-30 after the first infection. Putative ESC-like colonies were mechanically picked and expanded for subsequent validation. Established iPSC colonies were maintained on MEFs in DMEM/F12 medium supplemented with Glutamax, 20% knockout serum replacer, 1% NAA, 0.1 mmol/L βME and 50 ng/ml bFGF. Cells were passaged by manual dissection of cell clusters every 5-6 days. If not stated otherwise, all cell culture reagents were obtained from Gibco/Invitrogen. The human iPS cell line derived from foreskin fibroblasts, clone 1 (iPSC1), was kindly provided by James Thomson (University of Wisconsin, Madison, WI, USA) [38]. Human ES cell lines H1, H9 and HES-2 (WiCell Research Institute, Madison, WI, USA) were used as controls. Work with human ES cells has been approved by the regulatory authorities at the Robert Koch Institute, Berlin, Germany (permit number 1710-79-1-4-2-A10).

Cardiac differentiation

Cardiac differentiation of human iPS and ES cells was carried out on the murine visceral endoderm-like cell line END2 in Knockout-DMEM containing 1 mM L-glutamine, 1% NAA, 0.1 mmol/L βME and Penicillin/Streptomycin as described earlier [4, 39]. The co-culture was left undisturbed at 37°C for 4 days. First medium change was performed on day 5 and later on days 9, 12 and 15 of differentiation. Spontaneously contracting clusters or single cardiomyocytes were used for experiments on day 20-30 of differentiation.

RT-PCR and quantitative RT-PCR

Total RNA was isolated using TRIzol Reagent (Invitrogen) and cDNA was synthesized for semiquantitative or quantitative RT-PCR as described previously [4]. For semiquantitative RT-PCR cDNA was amplified using JumpStart™ RedTaq ReadyMix™ PCR Reaction Mix (Sigma). For quantitative RT-PCR the cDNA samples were amplified using SYBR Green PCR Master Mix (Qiagen). *GAPDH* PCR-product was used as a reference. Primers are listed in Table 1.

Gene	Primer	Sequence (5′ to 3′)	Chromosomal localization (bp)[b]	Number and position (relative to TSS) of analyzed CpGs
NANOG	forward	GGAATATGGTTTAATAGGAATGGGATAA	chromosome 12 (7,941,610 − 7,941,761)	3 (-296, -300, -302)
	reverse[a]	CCAAACTAATTTCAAACTCCTAACTTC		
	sequencing	TTTTAAAAATTAAGAAAAAGGT		
OCT4 assay 1	forward	AAGTTTTTGTGGGGGATTTGTAT	chromosome 6 (31,138,482 − 31,138,667)	1 (-159)
	reverse[a]	CCACCCACTAACCTTAACCTCTA		
	sequencing	TGAGGTTTTGGAGGG		
OCT4 assay 2	forward	GGGTTTTGGAAGTTTAGTTAGG	chromosome 6 (31,138,275 − 31,138,445)	2 (+92, +84)
	reverse[a]	CAAACCCTCATTTCACCAA		
	sequencing	ATTTTTATTATTTGGAGGGG		

Table 2. Genes and primers used for bisulfite pyrosequencing. [a]biotinylated primer. [b]according to Ensembl release 62 - April 2011 (based on: Homo sapiens high coverage assembly GRCh37 from the Genome Reference Consortium). TSS, transcription start site.

Immunocytochemistry

Undifferentiated hES and iPS cells were fixed with 4% paraformaldehyde, permeabilized with 0.1% Triton X-100 and blocked with 5% FBS and then stained overnight at 4°C with primary antibodies against SOX2, NANOG (Stemgent), TRA-1-60 (BD Pharmingen), OCT4, TRA-1-80 or SSEA4 (Santa Cruz). Nuclei were counterstained with Hoechst 33342. Samples were embedded in ProLong Gold antifade reagent (Invitrogen) and observed on an Axiovert Microscope (Carl-Zeiss) equipped with the image processing software Axiovision 4.5. Beating areas from differentiations of hES and iPS cell cultures were microdissected on day 25 of differentiation and dissociated into single cells by trypsinization. Single cardiomyocytes were plated on μ-dishes 35 mm, low (Ibidi GmbH) coated with fibronectin (2.5 μg/ml). 3-5 days after plating, the cells were fixed with 4% paraformaldehyde and stained as described above with anti-sarcomeric actinin (Sigma-Aldrich) and anti-RYR2 (Santa Cruz).

Bisulphite pyrosequencing

Genomic DNA was isolated from indicated cells using the DNeasy Blood and Tissue Kit (Qiagen) and bisulfite treatment was performed using the EpiTect Bisulfite Kit (Qiagen). The methylation status of the promoters of *OCT4* and *NANOG* was analyzed by bisulfite pyrosequencing on a PSQTM 96MA Pyrosequencing System (Biotage, Uppsala, Sweden) with the PyroGold SQA reagent kit (Biotage) [40]. Primers for bisulfite pyrosequencing are listed in Table 2. Pyro Q-CpG software (Biotage) was used for data analysis.

Microsatellite analysis

Genotype analysis of cell lines was performed using 12 highly informative microsatellite markers (D16S2621, D17S1303, D18S70, D18S976, D19S840, D1S466, D20S887, D22S280, D3S1768, D4S2632, D6S1045 and GAAT1A4). Fluorescently labelled PCR products were electrophoresed and detected on an automated 3730 DNA Analyzer and data were analyzed using Genemapper software version 3.0 (Applied Biosystems).

Karyotyping

Cytogenetic analysis was performed using standard Q-banding chromosome analysis by the certified cytogenetic laboratory of the Institute for Human Genetics (University of Mainz, Germany) according to standard procedures [41].

Teratoma assay

iPS cells (2-3×10^{6} cells/mouse) were injected as cell clumps subcutaneously into immunodeficient Rag2$^{-/-}$γ$_c^{-/-}$ mice obtained from Mamoru Ito (Institute for Experimental Animals, Tokyo, Japan). Teratomas were formed about 5-7 weeks later and consisted mostly of tissues and some cysts. Tumors were fixed in 4% paraformaldehyde, embedded in paraffin and later subjected to histological analysis by H&E staining.

Recording of action potentials

Action potentials (APs) of spontaneously beating single cardiomyocytes were measured using the whole-cell current clamp technique (EPC-9 amplifier and the PULSE software package, Heka Elektronik, Lambrecht, Germany). Microdissected beating clusters (BCs) were enzymatically dissociated with collagenase B at day 20-30 of differentiation and single CMs were plated onto glass cover slips and incubated for 48 hours prior to measurements. Cell membrane capacitance was determined on-line. Experiments were performed at 37°C in standard extracellular solution containing (in mM) 140 NaCl, 5.4 KCl, 1.8 CaCl$_2$, 1 MgCl$_2$, 10 HEPES and 10 D-Glucose (pH adjusted to 7.40 at 37°C with NaOH). Patch-clamp pipettes were filled with intracellular solution containing (in mMol/l) 50 KCl, 80 K-Aspartate, 1 MgCl$_2$, 3 Mg-ATP, 10 EGTA and 10 HEPES (pH adjusted to 7.40 with KOH). Isoproterenol (Iso) containing solutions were prepared freshly before the experiments, and applied using gravitational flow for 2 min prior to data collection. Electrophysiological data was analyzed using custom made software.

Multi-Electrode Array (MEA) measurements

Extracellular recordings of field potentials (FP) were performed using the 1060-Inv-BC amplifier and microelectrode

Fatima/Xu/Shao/Papadopoulos/Lehmann/Arnáiz-Cot/Rosa/Nguemo/
Matzkies/Dittmann/Stone/Linke/Zechner/Beyer/Hennies/Rosenkranz/
Klauke/Parwani/Haverkamp/Pfitzer/Farr/Cleemann/Morad/Milting/
Hescheler/Šarić

arrays (MEA) data acquisition system (Multichannel Systems, Reutlingen, Germany) as described previously [4, 42]. Beating clusters derived from iPS and ES cells were microdissected on day 20-30 of differentiation, plated on fibronectin (1 µg/ml)- and gelatine (0.1%)-coated MEA-plates and measured 24 hours after attachment. Standard measurements were performed at a sampling rate of 2 kHz in serum-free IMDM at 37°C. Data were analyzed off-line with MATLAB (The Mathworks, Natick, MA, USA). Home-made software based on LabView (National Instruments, Austin, TX USA) was used for analysis of interspike intervals (ISI). ISIs were defined as the time interval between two consecutive FP minima. The arrhythmicity of BCs before and after exposure to Iso (1 µM) was assessed by Poincare plots that allow visualization of long- and short-term beating variability.

Confocal measurements of Ca²⁺

Confocal imaging of voltage clamped cells was performed to record Ca^{2+} signals at a fixed potential (-60 mV or -80 mV) and to depolarize the membrane to activate I_{Ca} and thereby I_{Ca}-gated Ca^{2+} release. In conjunction with Ca^{2+} measurements the cells were voltage-clamped at room temperature (22-24°C) using a Dagan amplifier and pClamp (Clampex 10.2) software and the dialyzing pipette solution (in mM): 130 CsCl, 10 NaCl, 10 TeaCl, 5 Mg-ATP, 0.5 K_5Fluo-4, 10 D-Glucose and 10 HEPES (titrated to pH 7.2 with CsOH and Ca^{2+}-buffered to 150 or 200 nM using, repectively, additions of 0.2 mM Ca^{2+} or 0.6 mM Ca^{2+} together with 0.5 mM EGTA). The extracellular solution contained (in mM): 137 NaCl, 5.4 or 0 KCl, 1 $CaCl_2$, 1 $MgCl_2$, 10 D-Glucose and 10 HEPES (titrated to pH 7.4 with NaOH). Drugs dissolved in external solutions were rapidly (<50 ms) applied in close proximity to the cells using an electronically controlled multibarrelled puffing system the common outlet of which was placed in close proximity of the cell [43]. Application of 5-10 mM caffeine, 5 µM forskolin or 100 µM of 8-Br-cAMP (Sigma) in the external K⁺-free solutions was used to probe the cellular Ca^{2+} stores or spontaneous Ca^{2+} releases induced by phosphorylation of the RyR2. In voltage-clamped cells, confocal images of Ca^{2+}-dependent fluorescence were recorded at 0.1, 30, or 120 frames/s with a Noran Odyssey XL rapid two-dimensional laser scanning confocal microscopy system (Noran Instruments, Madison, WI) attached to a Zeiss Axiovert TV135 inverted microscope with a water-immersion objective lens (40×, NA 1.2, C-apochromate). The 488 nm line of an argon ion laser was used for excitation while emission was measured at > 515 nm. Non-dialyzed cells were examined confocally in the line-scan mode. Cells loaded with Fluo-4AM (5 µM for 15 min at 22-24°C) in Tyrode's solution (in mM: 140 NaCl, 1 $MgCl_2$, 5.4 KCl, 2 $CaCl_2$, 10 D-Glucose, 10 HEPES, 2 Na-Pyruvate) were transferred to the stage of an inverted Olympus FV1000 confocal microscope (488 nm excitation at 0.1% intensity, >505 nm emission).

Image analysis

The average resting fluorescence intensity (F_0) of 2-dimensional confocal fluorescence images of voltage-clamped, dialyzed cells was calculated from several frames measured immediately before drug application. Images were filtered by 4×4 pixel averaging. The amplitudes of the Ca^{2+}-dependent cellular fluorescence signals were quantified as $\Delta F/F_0 = F/F_0 - 1$, where F is the time-dependent and the F_0 is the average of several frames before or between the Ca^{2+} releases. F and F_0 were either integrated over the entire cell or were measured in specific regions. Line scans from non-dialyzed cells were background-corrected, 8-bit digitized, and analyzed graphically using a 3D surface plot routine (implemented in the ImageJ software, Wayne Rasband, NIH) thereby producing readouts of peak amplitude (F_{max}) *vs* base-line intensity (F_0) as an indicator of $[Ca^{2+}]_i$ as well as FDHM (Full Duration at Half Maximum).

Statistical analysis

Data are presented as mean ± standard error of mean (SEM). Statistical analyses were performed by two-tailed Student's t-test or paired t-test (p-value <0.05 was considered significant).

Results

Characterization of CPVT1-specific iPS cell lines

In order to generate CPVT1-specific iPS cells we have obtained a skin biopsy from a 46-year old woman with a diagnosis of CPVT1 (Fig. 1) who carried the missense mutation p.F2483I caused by a 7447T>A nucleotide substitution in exon 49 of *RYR2*. This mutation is localized in the FKBP12.6 binding domain of the RYR2 protein. Retroviral overexpression of the four transcription factors OCT4, SOX2, KLF4 and cMYC was used to induce pluripotency in healthy volunteer- and patient-derived dermal fibroblasts. Four different iPS cell clones (c1, c2, c5, and c6) were generated from CPVT fibroblasts and one clone (iPSC2) from normal fibroblasts. The presence of the patient-specific mutation was confirmed in CPVT iPS cells but not in control ones (Fig. 2a). All generated iPS cell lines presented a human ES cell-like colony morphology (Fig. 2b) and alkaline phosphatase activity (Fig. 2c). They expressed the endogenous pluripotency markers at the protein (Fig. 2d,e) and transcript level (Fig. 2f), and silenced the expression of retrovirally encoded reprogramming factors (Fig. 2g). The methylation pattern in promoter regions of *OCT4* and *NANOG* genes was undistinguishable from that of conventional ES cells in all CPVT-iPS cell lines (Fig. 2h), and the chromosomal structure was normal in a cytogenetic analysis (Fig. 2i). Furthermore, these iPS cells formed teratomas in immunodeficient mice, which consisted of derivatives of all three germ layers (Fig. 2j). Microsatellite analyses revealed that all iPS cell lines carried the same genotype as parental somatic cells, excluding the possibility of contamination with other ES

Fig. 1. ECG signs of CPVT in a patient with a mutation p.F2483I in the *RYR2* gene. The panel shows a 12-lead ECG of a CPVT1 patient during exercise, which is characterized by tachycardia and typical polymorphic ventricular extra beats (arrows). The ECG at rest was normal.

or iPS cell lines in our laboratories (data not shown).

Differentiation of CPVT1 iPS cells to cardiomyocytes

We used coculture with the murine visceral endoderm-like cell line END2 to differentiate CPVT1 and control iPS cells (iPSC1, iPSC2) as well as conventional human ES cells (H1, H9, HES2) to cardiomyocytes *in vitro*. All iPS and ES cell lines showed a comparable cardiac differentiation potential with approximately 20-23% of embryoid bodies giving rise to spontaneously contracting areas after 8-9 days of differentiation. Immunocytochemical staining for the sarcomeric Z-disc protein α-actinin revealed that CPVT1 cardiomyocytes display a somewhat disorganized pattern of cross-striations (Fig. 3a) typical of immature ES- or iPS-cardiomyocytes [4]. Costaining for RYR2 showed a spotted pattern of expression in the cytosol and in the perinuclear region adjacent but not explicitly localized to Z-bands (Fig. 3a), consistent with previous reports for human ESC-derived cardiomyocytes [44]. At the transcript level, microdissected beating clusters (BCs) derived from control cell lines and CPVT1 iPSCs expressed comparable levels of *RYR2, FKBP1B* (encoding for the FK-506 binding protein FKBP12.6)*, CASQ2* (encoding for cardiac calsequestrin) and

genes encoding several cardiac structural proteins (Fig. 3b). These data suggest that CPVT1 BCs contain cardiomyocytes with features similar to those of control cell lines.

Analysis of arrhythmicity of beating clusters

In order to study the characteristic arrhythmic propensity of CPVT1 patients in CPVT cardiomyocytes we first recorded field potentials from whole BCs that were plated on microelectrode arrays (MEA). MEA traces from 15 control BCs (10 iPS cell-derived and 5 ES cell-derived) and 22 BCs from three CPVT1 iPS cell subclones were analyzed using Poincarè plots to assess the variability of their interspike intervals at baseline and after stimulation with β-adrenergic agonist isoproterenol (Iso). Only 2 of 15 control BCs (13.3%) were arrhythmic prior to and after Iso application. In contrast, 5 of 22 (22.7%) CPVT BCs showed arrhythmic activity at basal conditions and 7 of 22 (31.8%) were arrhythmic upon Iso application. Although differences between control and CPVT BCs did not reach statistical significance, the higher tendency to arrhythmia of undissociated BCs from CPVT iPS cell clones as compared to control BCs at baseline and upon adrenergic stimulation suggest that cardiomyocytes within CPVT clusters may exhibit a disease-specific phenotype.
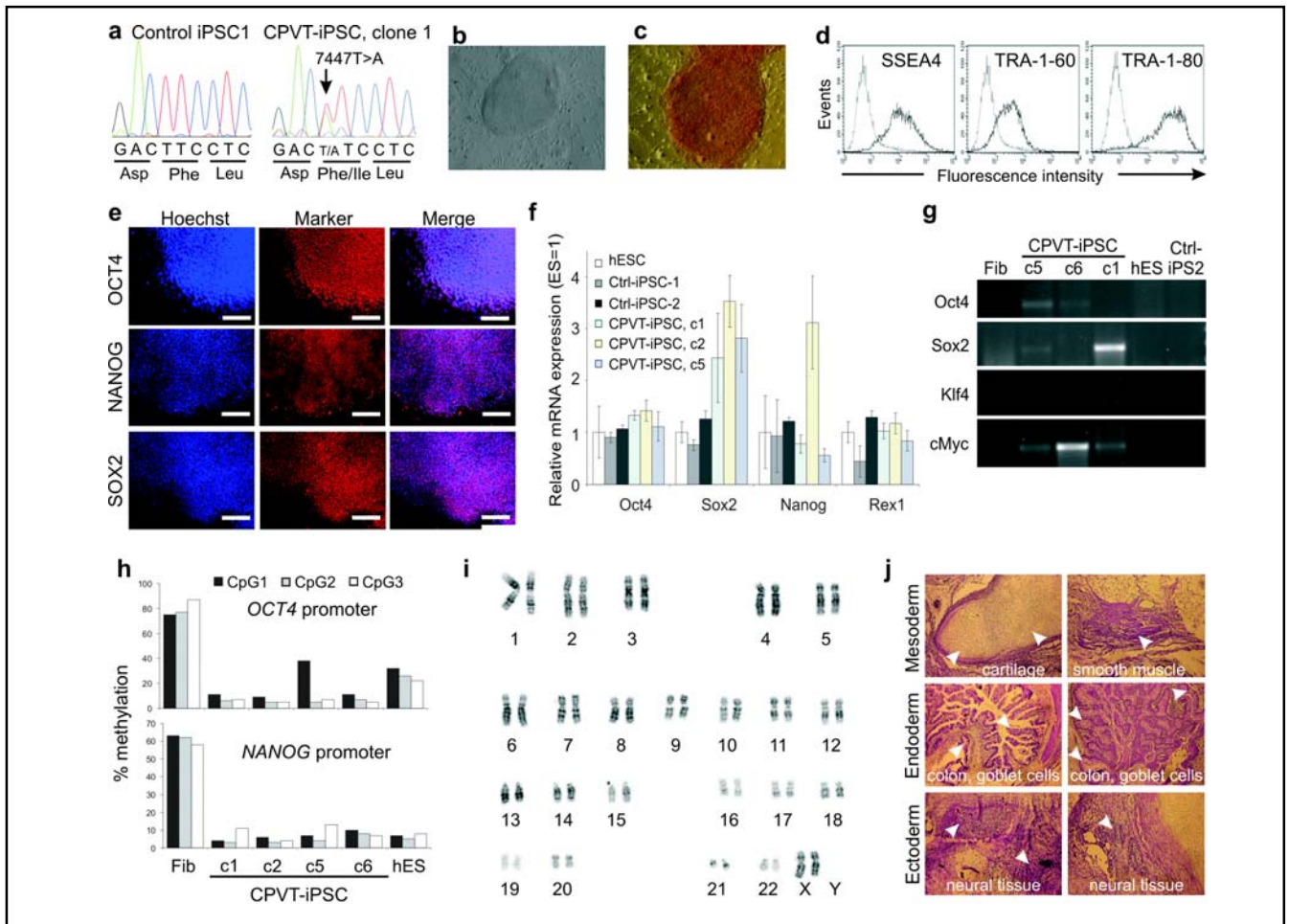
Fatima/Xu/Shao/Papadopoulos/Lehmann/Arnáiz-Cot/Rosa/Nguemo/
Matzkies/Dittmann/Stone/Linke/Zechner/Beyer/Hennies/Rosenkranz/
Klauke/Parwani/Haverkamp/Pfitzer/Farr/Cleemann/Morad/Milting/
Hescheler/Šarić

Fig. 2. Characterization of CPVT1 iPS cells. (a) Verification of *RYR2* mutation p.F2483I by DNA sequencing in CPVT1 iPS cells. (b) Human ES cell-like morphology of an CPVT iPS cell colony. (c-e) Expression of pluripotency markers on CPVT1 iPS cells (clone 1) as determined by alkaline phosphatase staining (c) flow cytometry (d) and immunocytochemistry (e). Scale bars, 400 μm. (f) Expression of pluripotency markers at transcript level as determined by qRT-PCR. Expression values were normalized to *GAPDH* and are presented as mean ± S.E.M. (n=3) relative to corresponding transcript levels in human ES cells. Endogenous markers *NANOG* and *REX1*, which were not expressed from the retroviral reprogramming cassette, are expressed in iPS cells at levels similar to those in the conventional ES cell line HES2. (g) Silencing of the retroviral transgenes in CPVT1 and control iPS cell lines as determined by semiquantitative RT-PCR. Human ES cells (hES) and donor fibroblasts (Fib) were used as a negative control. (h) Methylation levels of promoter regions of *OCT4* and *NANOG* in CPVT1 fibroblasts (Fib), four subclones of CPVT1 iPS cells and human ES cell line HES2. (i) Cytogenetic analysis of CPVT1 iPS cells reveals that they have normal karyotype. (j) H&E-stained paraffin sections of CPVT1 iPS cell-derived teratoma showing formation of tissue derivatives of all three germ layers (arrowheads).

Action potentials from control and CPVT1-iPS cell-derived cardiomyocytes

The electrophysiological hallmark of cardiomyocytes expressing CPVT1 associated RYR2 mutations are delayed afterdepolarizations (DADs) that occur after adrenergic stimulation [45-47]. To determine whether the *RYR2* mutation described above causes this typical disease phenotype, the whole-cell patch clamp method was used to record action potentials (APs) in single cardiomyocytes before and after Iso treatment. All control and CPVT1 cell lines gave rise to comparable numbers of nodal-, atrial- and ventricular-like cells (Fig. 4) and the AP parameters of cardiomyocytes derived from three different clonal CPVT iPS cell sublines were indistinguishable from each other as well as from control ES and iPS cell-derived cardiomyocytes (data not shown). All of 32 control cardiomyocytes (20 ES cell- and 12 iPS cell-derived) showed the expected positive chronotropic response to 1 μM Iso without generating arrhythmia (Fig. 5a,b). In contrast, 22 out of 38 CPVT cardiomyocytes (57.9%) showed
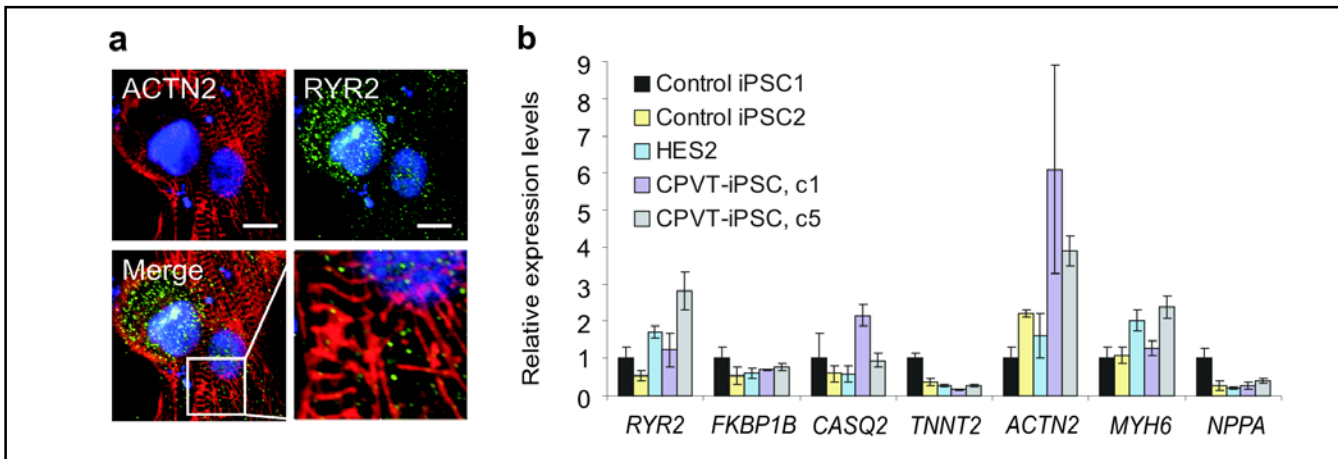
Fig. 3. Generation of cardiomyocytes from CPVT1 iPS cells. (a) Confocal images of CPVT1-cardiomyocytes stained with α-actinin (red) and RYR2 (green) antibodies and counterstained with Hoechst 33342 (blue). Inset: high magnification merged image of α-actinin-stained Z-bands and RYR2. Scale bar, 10 μm. (b) Quantitative RT-PCR analysis demonstrating expression of indicated genes in microdissected spontaneously contracting areas differentiated from human ES cell line HES2, two control and two CPVT1 iPS cell lines.
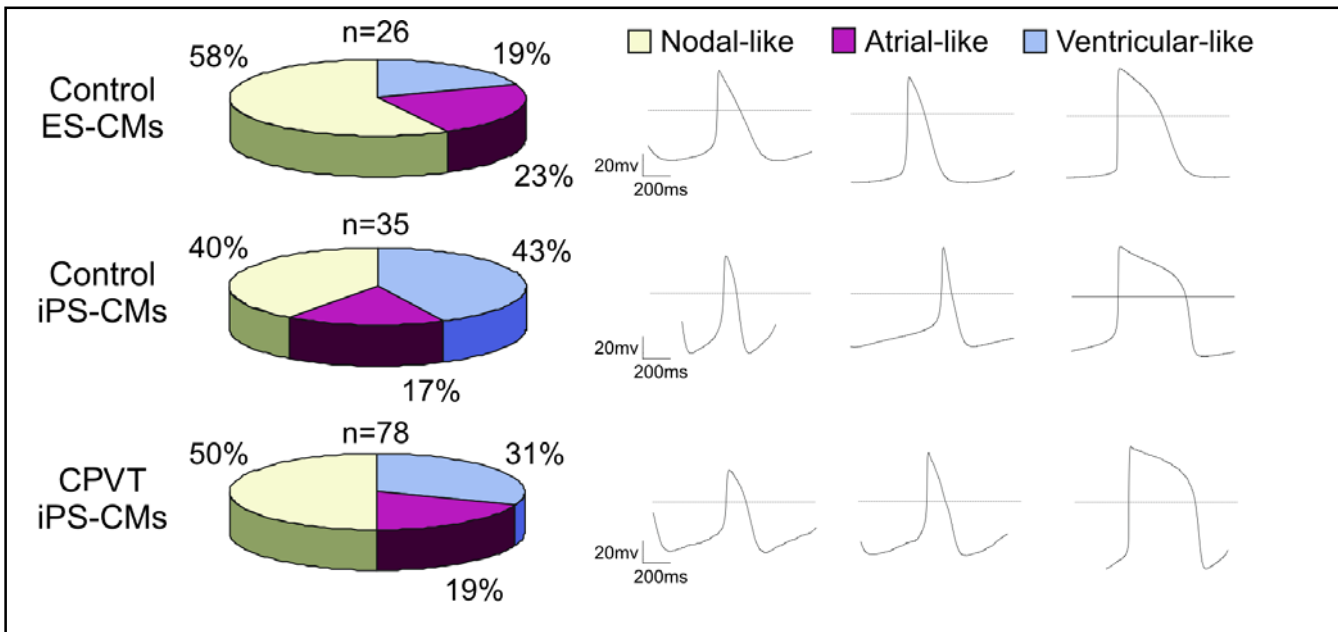

Fig. 4. Characterization of cardiac cell types derived from control ES and iPS cells and CPVT1 iPS cells. Action potentials (APs) in single cardiomyocytes differentiated from control ES and iPS cells and CPVT1 iPS cells were analyzed by the whole-cell patch clamp method. The frequencies of the three main cardiac cell types in control ES and iPS cells as well as CPVT1 iPS cell lines are similar. The classification of different cardiac cell types was based on the morphology of APs (right panels) and AP parameters V_{max} (~10 V/sec for atrial and ventricular cardiomyocytes, ~5 V/sec for nodal cardiomyocytes) and APD90/APD50 (~2 for atrial and <1.5 for ventricular).

negative chronotropy to Iso applications and 13 out of 38 RYR2-mutant cells (34.2%) developed arrhythmia and putative DADs upon Iso application (Fig. 5c,d,e). These responses were consistently recorded in cardiomyocytes derived from all three clonal CPVT sublines. The occurrence of DADs in a large fraction of CPVT cardiomyocytes indicates that these cells recapitulate the disease-specific abnormalities seen in CPVT patients [46] and animal models of this disease [48].

Fatima/Xu/Shao/Papadopoulos/Lehmann/Arnáiz-Cot/Rosa/Nguemo/
Matzkies/Dittmann/Stone/Linke/Zechner/Beyer/Hennies/Rosenkranz/
Klauke/Parwani/Haverkamp/Pfitzer/Farr/Cleemann/Morad/Milting/
Hescheler/Šarić

Fig. 5. Electrophysiological characterization of control and CPVT1 cardiomyocytes. Action potentials (APs) in single cardiomyocytes were recorded by the whole-cell patch clamp method in the current-clamp mode and the beating frequency of cells at basal state and after 1 μM isoproterenol (Iso) treatment was determined. Cardiomyocytes differentiated from control ES (a) and iPS cell lines (b) responded to 1 μM Iso stimulation with positive chronotropy and did not show any arrhythmia after treatment. Representative traces of APs before and after Iso treatment are shown in the middle and right panels, respectively. (c) Large fraction of cardiomyocytes (22 out of 38 cells, 57.9%) derived from CPVT1 iPS cells reacted to Iso with negative chronotropy (left panel) and 13 out of 38 (34.2%) CPVT1 cardiomyocytes exhibited arrhythmia and putative DADs (arrows above traces in the right panel). (d,e) Representative traces of arrhythmic action potentials in two additional cells stimulated with Iso. The AP traces in the cell depicted in panel (d) show putative DADs (arrows). The n-values in panels (a-c) show the total number of analyzed cells. Error bars show s.e.m.. *P<0.05, **P<0.01.
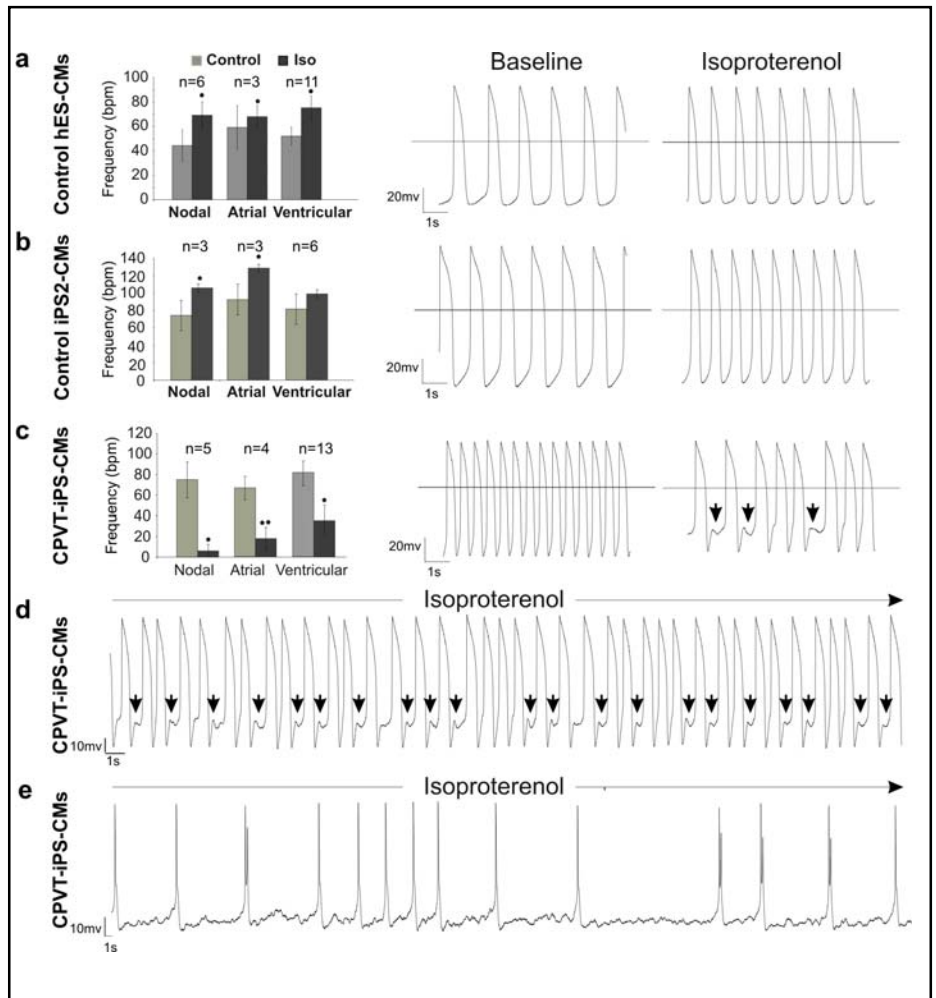
Calcium handling in control and CPVT1-iPS cell-derived cardiomyocytes

It is widely accepted that DADs and subsequent arrhythmias in RYR2-mutant cardiomyocytes are caused by uncontrolled Ca^{2+} release from the SR during diastole [36]. In order to detect Ca^{2+} handling abnormalities in spontaneously beating CPVT1 cardiomyocytes, we used confocal fluorescence imaging under the line-scan mode to analyze local Ca^{2+} release events in cells loaded with the Ca^{2+} indicator Fluo-4. These analyses showed that CPVT cardiomyocytes exhibit higher amplitudes (Fig. 6a) and longer durations (Fig. 6b) of spontaneous local Ca^{2+} release events (Fig. 6c) already at basal state. These observations are consistent with aberrant SR Ca^{2+} release in cells expressing mutant RYR2 that underlie CPVT1 [33, 34].

To gain further insight into Ca^{2+} handling abnormalities in CPVT1 cardiomyocytes under more controlled conditions, cells were voltage-clamped in the whole cell configuration and the sarcolemmal Ca^{2+} currents (I_{Ca}) activated by depolarizing pulses and Ca^{2+} transients were measured by confocal microscopy. Calcium stores in CPVT1 cardiomyocytes were robust and could be released by caffeine (data not shown). When the cells were depolarized from -60 mV to 0 mV large I_{Ca} (~8-10 pA/pF) accompanied by rapidly activating Ca^{2+} transients were observed in CPVT1 cardiomyocytes (Fig. 6d-f). Although robust Ca-transients were triggered by activation of I_{Ca} (Ca^{2+} induced Ca^{2+} release, CICR) at 0 mV and by I_{Ca} tail currents on repolarizations from positive potentials (>+60 mVs), it was also consistently noted that the Ca^{2+} release from internal Ca^{2+} stores continued long after repolarization of the membrane (Fig. 6f). Consistent with the slow decay of global Ca^{2+} transients following the depolarizing pulses, we regularly observed a steep rise in cytosolic Ca^{2+} when cells were exposed to 5 μM forskolin (Fig. 6g) or 100 μM 8-Br-cAMP (not shown), that were sustained and appeared not to be reversible.
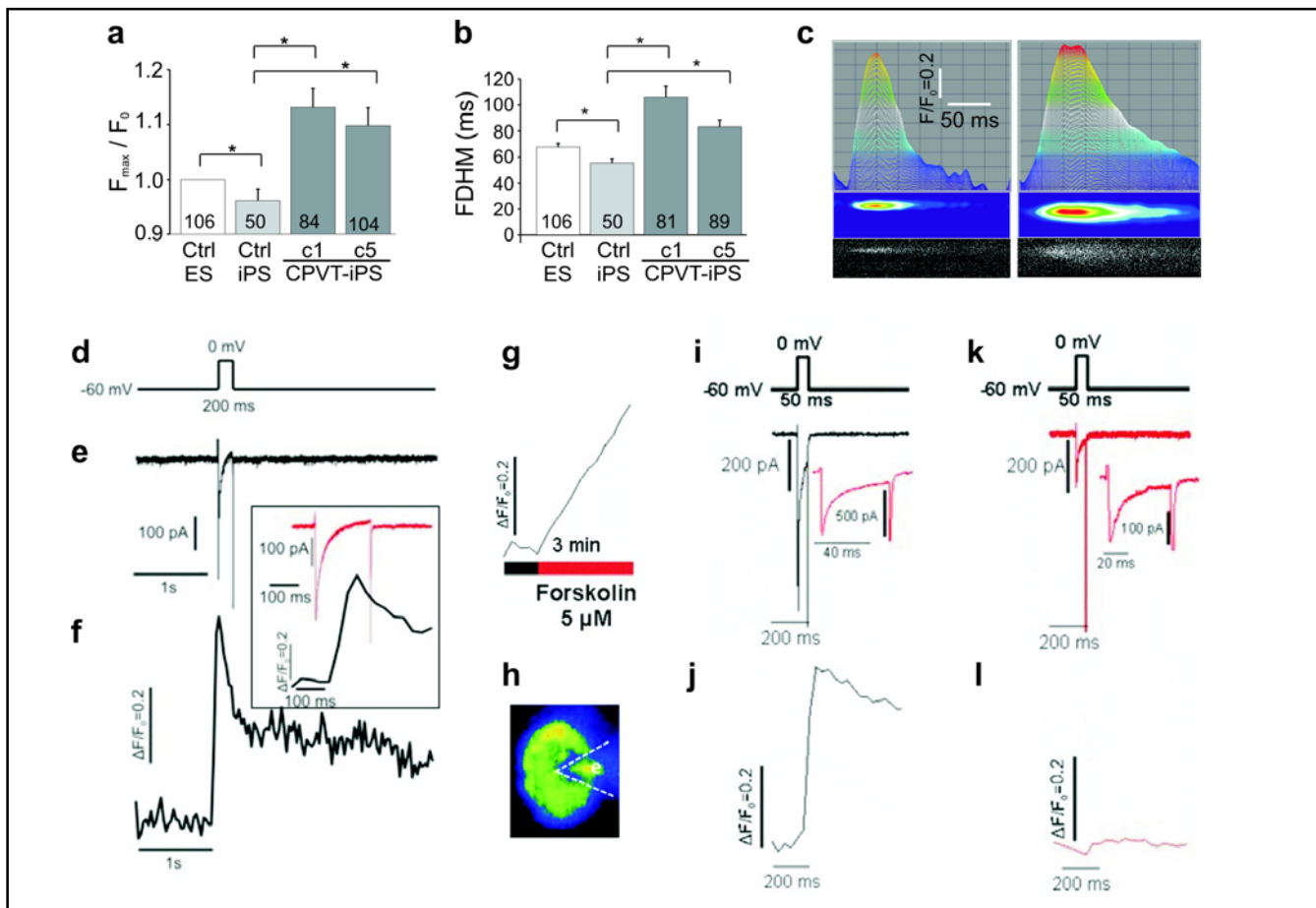
Fig. 6. Calcium handling in control and CPVT1 iPS cell-derived cardiomyocytes. (a-f) Magnitude (a) and full duration at half amplitude (b, FDHM) of 50-106 local diastolic Ca^{2+} release events measured in the line-scan mode in control (clone 1) and CPVT1 iPS cell-derived cardiomyocytes (clones 1 and 5). Error bars show S.E.M.. *P<0.05. (c) Sample line-scan recordings of local Ca^{2+}-release events in control iPSC2 (left) and CPVT1 cardiomyocytes (right) showing time-dependence of maximal fluorescence intensity (top), processed color-coded intensity distribution (middle), and measured distribution of Ca^{2+}-dependent fluorescence (bottom). (d-f) Simultaneous recordings of the membrane current (e) and the cellular average of the I_{Ca}-gated Ca^{2+} release ($\Delta F/F_0$, f) in a voltage-clamped CPVT1 cardiomyocyte (clone 1) that was depolarized from -60 mV to 0 mV for 200 ms (d). The inset shows the membrane current and the initial fluorescence spike on an expanded time scale. (g-l) In voltage clamped CPVT1-iPS cell-derived cardiomyocytes (clone 1), forskolin (3 min, 5 μM) caused elevation of baseline Ca^{2+} (g) and suppression of I_{Ca}-activated Ca^+ transients (l vs j) without a concurrent suppression of I_{Ca} (k vs i). (h) Fluorescence image of the cell and voltage-clamp (dotted line) as seen at frame rates of 30 Hz (j and l) or 0.1 Hz (g). Insets in panels (i) and (k) show current traces on an expanded time scale.

The decrease in I_{Ca} (panel i vs. k) and Ca^{2+}-transients (panel j vs. l) observed in the presence of forskolin was most likely related to the large and sustained rise of cytosolic Ca^{2+}, which also was accompanied by a reduction in the caffeine-induced Ca^2 release (not shown) suggesting depletion of the RyR2-gated Ca^{2+} stores.

Discussion

In this study we have generated iPS cell lines from a patient with CPVT1 carrying a novel mutation in the FKBP12.6-binding region of RYR2. Frequent DADs and arrhythmias in CPVT cardiomyocytes exposed to adrenergic agonists were consistently observed. These DADs closely resemble the DADs that were observed on endocardial monophasic action potential recordings in intact hearts of CPVT patients after isoproterenol infusion [46, 47] and those recorded in isoproterenol-stimulated ventricular myocytes isolated from a mouse model of CPVT harboring a R4496C mutation in *RYR2* [48]. Global cytosolic Ca^{2+} transients were irregular in a fraction of Iso-treated cells and local Ca^{2+}-releases were of higher amplitudes and longer durations compared to control cells.

Fatima/Xu/Shao/Papadopoulos/Lehmann/Arnáiz-Cot/Rosa/Nguemo/
Matzkies/Dittmann/Stone/Linke/Zechner/Beyer/Hennies/Rosenkranz/
Klauke/Parwani/Haverkamp/Pfitzer/Farr/Cleemann/Morad/Milting/
Hescheler/Šarić

Depolarizing clamp pulses produced cytosolic Ca^{2+} increases that continued to rise even after I_{Ca} was deactivated on repolarization of the membrane. Of direct relevance to the clinical translational implication of this *RYR2* mutation, we found an abnormal Ca^{2+} response to phosphorylation induced by increased cAMP levels where cells appeared to have poorly regulated global Ca^{2+} releases that were followed by failure of CICR in the phosphorylated cells. The occurrence of DADs and arrhythmias on Iso exposure, abnormal sensitivity to phosphorylation and cAMP-mediated regulation, the tendency for I_{Ca}-triggered Ca^{2+} release to continue following repolarization were all consistent with the idea that this particular *RYR2* mutation may increase the open probability of RYR2 especially upon adrenergic stimulation thus making patients carrying this mutation susceptible to ventricular tachycardia [47].

The central event regulating cardiac muscle contraction is a rapid transient elevation of cytosolic Ca^{2+} resulting from CICR. In this process, depolarizing action potential (AP) induces a small influx of Ca^{2+} through the plasmalemmal voltage-gated calcium channels ($Ca_V1.2$), triggering, in turn, cytosolic release of Ca^{2+} from the SR into the cytosol through RYR2. Ca^{2+}-release *via* RYR2 is regulated by several physiological mechanisms. One potential mechanism includes the FK-506 binding protein (FKBP12.6, also known as calstabin 2), which binds to the cytosolic surface of each RYR2 monomer and stabilizes the closed state of a homotetrameric RYR2 channel [49]. It has been proposed that protein kinase A-induced RYR2 phosphorylation leads to dissociation of FKBP12.6 from the RYR2 complex, increasing the open probability of the channel and sensitivity to Ca^{2+}-dependent activation [50]. Wehrens and colleagues proposed that RYR2 mutants reduce the binding affinity of RYR2 for the regulatory protein FKBP12.6, which worsens when RYR2 is phosphorylated upon adrenergic stimulation and promotes Ca^{2+} leakage from the SR [51, 52]. The molecular mechanism by which the novel RYR2 mutation p.F2483I described in this study alters the activity of RYR2 is not clear. Since this mutation is localized in the FKBP12.6-binding region of RYR2 it may destabilize the interaction of this stabilizing protein with RYR2 and contribute to the disease phenotype. By using the iPS cell-based CPVT1 model the molecular mechanism of electrophysiological abnormalities can be studied. Experimental compounds such as K201, a derivative of 1,4-benzothiazepine formerly called JTV519 [52, 53] and its more selective RYR2-specific derivative S107 [54] enhance the binding of FKBP12.6 to the mutant RYR2 and could be used to probe the mechanism of the disease in this model.

Since adrenergic stimulation is critical in triggering arrhythmia, beta-blockers are considered as the mainstay of CPVT therapy [55, 56]. However, the fact that about 30% of CPVT patients taking β-blockers depend on implantable cardioverter-defibrillator to prevent life-threatening arrhythmias emphasizes the need for better understanding the mechanism of this disease and the identification of new more potent drugs. The CPVT1 iPS cell derived-cardiomyocytes described in this study represent a unique platform that can be used for drug screening and development of optimized patient-tailored therapies. In addition to beta-blockers, this *in vitro* system could be used for testing other promising drugs such as flecainide, dantrolene and carvedilol. Flecainide, a class Ic antiarrhythmic drug, may have the ability to support the antiadrenergic effect of beta-blockers, because it has been shown to prevent arrhythmia in CPVT patients and RYR2 mutant mouse models. This effect is most likely mediated by reducing the availability of sodium channels in the plasma membrane [57] or by directly blocking RYR2 in the SR [58]. Dantrolene, a drug normally used for treatment of malignant hyperthermia due to its ability to block skeletal RYR1, was also found to inhibit Ca^{2+} leak through the cardiac RYR2 by correcting the defective inter-domain interaction between N-terminal and central (harboring FKBP12.6 binding region) domains of RYRs [59]. These authors also showed that dantrolene prevented ventricular tachycardia in knock-in mice bearing the human R2474S RYR2 mutation, but its applicability in clinical setting has not yet been investigated. In a recent report Zhou and coworkers have demonstrated that carvedilol, a non-selective beta- (β1/β2) and alpha (α1)-blocker, also directly acts on RYR2 by reducing its open probability and spontaneous Ca^{2+} waves [60]. Its new synthetic analog VK-II-86 prevented stress-induced ventricular tachyarrhythmias in RYR2-mutant mice, but its effect in CPVT patients has not been well assessed. Therefore, the use of iPS cell-based human models carrying the genetic constitution of each particular patient will increase the predictive power of *in vitro* drug testing and has the potential to overcome limitations inherent to animal models of human heart diseases and surrogate cell culture systems [61].

The potential of the iPS cell-based models for studying the disease mechanism and predicting drug efficacy will greatly depend on further improvements in the reprogramming technology and on optimized cardiac differentiation and maturation protocols. The iPS cell lines used in this study contain sequences of reprogramming

transgenes stably integrated into their genome at random sites. We have observed that exogenous SOX2 and c-MYC were partially reactivated in some iPS cell clones. This phenomenon alone or together with the insertional mutagenesis by retroviruses may have caused the variability that we have observed in the expression of pluripotency markers SOX2 and NANOG between different clones of undifferentiated iPS cells as well as the differences in the expression of some cardiac specific markers in different clones of iPS cell-derived beating clusters. It is also possible that ectopic expression of retroviral reprogramming factors or deregulation of gene expression by retroviral insertions could affect functional properties of iPS cell-derivatives. This notion is supported by observation that iPS cells generated by non-integrating reprogramming methods are transcriptionally more similar to ES cells than those generated with stably integrating viral vectors [62]. Therefore, reprogramming methods that allow generation of genetically intact iPS cell lines should be favoured for establishment of disease models in future studies. However, it is very likely that even in such cell lines there will be still a certain degree of variability in gene expression profiles and differentiation capacities of different iPS cell lines and functional properties of their differentiated derivatives. It is well known that this variability exist even between different human ES cell lines as well as ES and iPS cell-derived cardiomyocytes [9, 63]. Therefore, the limitation that variation between the clones could impose on use of iPS cells for disease modelling could also be overcome by including sufficient numbers of control and diseased iPS cell lines for functional studies, as we have done in this report.

In conclusion, we have established the first *in vitro* human iPS cell-based model of CPVT1 and demonstrate that iPS cell-derived cardiomyocytes with RYR2 mutation reported here reflect the Ca^{2+} signalling phenotype of CPVT1 patients and provide a new platform for investigating the mechanism underlying this disease and its pharmacotherapy.

References

1 Takahashi K, Tanabe K, Ohnuki M, Narita M, Ichisaka T, Tomoda K, Yamanaka S: Induction of pluripotent stem cells from adult human fibroblasts by defined factors. Cell 2007;131:861-872.

2 Nelson TJ, Martinez-Fernandez A, Terzic A: Induced pluripotent stem cells: developmental biology to regenerative medicine. Nat Rev Cardiol 2010;7:700-710.

3 Vitale AM, Wolvetang E, Mackay-Sim A: Induced pluripotent stem cells: a new technology to study human diseases. Int J Biochem Cell Biol 2011;43:843-846.

4 Gupta MK, Illich DJ, Gaarz A, Matzkies M, Nguemo F, Pfannkuche K, Liang H, Classen S, Reppel M, Schultze JL, Hescheler J, Saric T: Global transcriptional profiles of beating clusters derived from human induced pluripotent stem cells and embryonic stem cells are highly similar. BMC Dev Biol 2010;10:98.

5 Germanguz I, Sedan O, Zeevi-Levin N, Shtreichman R, Barak E, Ziskind A, Eliyahu S, Meiry G, Amit M, Itskovitz-Eldor J, Binah O: Molecular characterization and functional properties of cardiomyocytes derived from human inducible pluripotent stem cells. J Cell Mol Med 2011;15:38-51.

6 Gai H, Leung EL, Costantino PD, Aguila JR, Nguyen DM, Fink LM, Ward DC, Ma Y: Generation and characterization of functional cardiomyocytes using induced pluripotent stem cells derived from human fibroblasts. Cell Biol Int 2009;33:1184-1193.

7 Yokoo N, Baba S, Kaichi S, Niwa A, Mima T, Doi H, Yamanaka S, Nakahata T, Heike T: The effects of cardioactive drugs on cardiomyocytes derived from human induced pluripotent stem cells. Biochem Biophys Res Commun 2009;387:482-488.

Fatima/Xu/Shao/Papadopoulos/Lehmann/Arnáiz-Cot/Rosa/Nguemo/ Matzkies/Dittmann/Stone/Linke/Zechner/Beyer/Hennies/Rosenkranz/ Klauke/Parwani/Haverkamp/Pfitzer/Farr/Cleemann/Morad/Milting/ Hescheler/Šarić

8 Tanaka T, Tohyama S, Murata M, Nomura F, Kaneko T, Chen H, Hattori F, Egashira T, Seki T, Ohno Y, Koshimizu U, Yuasa S, Ogawa S, Yamanaka S, Yasuda K, Fukuda K: In vitro pharmacologic testing using human induced pluripotent stem cell-derived cardiomyocytes. Biochem Biophys Res Commun 2009;385:497-502.

9 Zhang J, Wilson GF, Soerens AG, Koonce CH, Yu J, Palecek SP, Thomson JA, Kamp TJ: Functional cardiomyocytes derived from human induced pluripotent stem cells. Circ Res 2009;104:e30-41.

10 Mehta A, Chung YY, Ng A, Iskandar F, Atan S, Wei H, Dusting G, Sun W, Wong P, Shim W: Pharmacological response of human cardiomyocytes derived from virus-free induced pluripotent stem cells. Cardiovasc Res 2011;91:577-586.

11 Dimos JT, Rodolfa KT, Niakan KK, Weisenthal LM, Mitsumoto H, Chung W, Croft GF, Saphier G, Leibel R, Goland R, Wichterle H, Henderson CE, Eggan K: Induced pluripotent stem cells generated from patients with ALS can be differentiated into motor neurons. Science 2008;321:1218-1221.

12 Soldner F, Hockemeyer D, Beard C, Gao Q, Bell GW, Cook EG, Hargus G, Blak A, Cooper O, Mitalipova M, Isacson O, Jaenisch R: Parkinson's disease patient-derived induced pluripotent stem cells free of viral reprogramming factors. Cell 2009;136:964-977.

13 Zhang N, An MC, Montoro D, Ellerby LM: Characterization of Human Huntington's Disease Cell Model from Induced Pluripotent Stem Cells. PLoS Curr 2010;2:RRN1193.

14 Marchetto MC, Carromeu C, Acab A, Yu D, Yeo GW, Mu Y, Chen G, Gage FH, Muotri AR: A model for neural development and treatment of Rett syndrome using human induced pluripotent stem cells. Cell 2010;143:527-539.

15 Ku S, Soragni E, Campau E, Thomas EA, Altun G, Laurent LC, Loring JF, Napierala M, Gottesfeld JM: Friedreich's ataxia induced pluripotent stem cells model intergenerational GAATTC triplet repeat instability. Cell Stem Cell 2010;7:631-637.

16 Chang T, Zheng W, Tsark W, Bates SE, Huang H, Lin RJ, Yee JK: Phenotypic Rescue of Induced Pluripotent Stem Cell-Derived Motoneurons of a Spinal Muscular Atrophy Patient. Stem Cells 2011;in press.

17 Brennand KJ, Simone A, Jou J, Gelboin-Burkhart C, Tran N, Sangar S, Li Y, Mu Y, Chen G, Yu D, McCarthy S, Sebat J, Gage FH: Modelling schizophrenia using human induced pluripotent stem cells. Nature 2011;473:221-225.

18 Zou J, Sweeney CL, Chou BK, Choi U, Pan J, Wang H, Dowey SN, Cheng L, Malech HL: Oxidase-deficient neutrophils from X-linked chronic granulomatous disease iPS cells: functional correction by zinc finger nuclease-mediated safe harbor targeting. Blood 2011;117:5561-5572.

19 Rashid ST, Corbineau S, Hannan N, Marciniak SJ, Miranda E, Alexander G, Huang-Doran I, Griffin J, Ahrlund-Richter L, Skepper J, Semple R, Weber A, Lomas DA, Vallier L: Modeling inherited metabolic disorders of the liver using human induced pluripotent stem cells. J Clin Invest 2010;120:3127-3136.

20 Ghodsizadeh A, Taei A, Totonchi M, Seifinejad A, Gourabi H, Pournasr B, Aghdami N, Malekzadeh R, Almadani N, Salekdeh GH, Baharvand H: Generation of liver disease-specific induced pluripotent stem cells along with efficient differentiation to functional hepatocyte-like cells. Stem Cell Rev 2010;6:622-632.

21 Lemonnier T, Blanchard S, Toli D, Roy E, Bigou S, Froissart R, Rouvet I, Vitry S, Heard JM, Bohl D: Modeling neuronal defects associated with a lysosomal disorder using patient-derived induced pluripotent stem cells. Hum Mol Genet 2011;20:3653-3666.

22 Tolar J, Park IH, Xia L, Lees CJ, Peacock B, Webber B, McElmurry RT, Eide CR, Orchard PJ, Kyba M, Osborn MJ, Lund TC, Wagner JE, Daley GQ, Blazar BR: Hematopoietic differentiation of induced pluripotent stem cells from patients with mucopolysaccharidosis type I (Hurler syndrome). Blood 2011;117:839-847.

23 Ye Z, Zhan H, Mali P, Dowey S, Williams DM, Jang YY, Dang CV, Spivak JL, Moliterno AR, Cheng L: Human-induced pluripotent stem cells from blood cells of healthy donors and patients with acquired blood disorders. Blood 2009;114:5473-5480.

24 Carvajal-Vergara X, Sevilla A, D'Souza SL, Ang YS, Schaniel C, Lee DF, Yang L, Kaplan AD, Adler ED, Rozov R, Ge Y, Cohen N, Edelmann LJ, Chang B, Waghray A, Su J, Pardo S, Lichtenbelt KD, Tartaglia M, Gelb BD, Lemischka IR: Patient-specific induced pluripotent stem-cell-derived models of LEOPARD syndrome. Nature 2010;465:808-812.

25 Moretti A, Bellin M, Welling A, Jung CB, Lam JT, Bott-Flugel L, Dorn T, Goedel A, Hohnke C, Hofmann F, Seyfarth M, Sinnecker D, Schomig A, Laugwitz KL: Patient-specific induced pluripotent stem-cell models for long-QT syndrome. N Engl J Med 2010;363:1397-1409.

26 Itzhaki I, Maizels L, Huber I, Zwi-Dantsis L, Caspi O, Winterstern A, Feldman O, Gepstein A, Arbel G, Hammerman H, Boulos M, Gepstein L: Modelling the long QT syndrome with induced pluripotent stem cells. Nature 2011;471:225-229.

27 Matsa E, Rajamohan D, Dick E, Young L, Mellor I, Staniforth A, Denning C: Drug evaluation in cardiomyocytes derived from human induced pluripotent stem cells carrying a long QT syndrome type 2 mutation. Eur Heart J 2011;32:952-962.

28 Yazawa M, Hsueh B, Jia X, Pasca AM, Bernstein JA, Hallmayer J, Dolmetsch RE: Using induced pluripotent stem cells to investigate cardiac phenotypes in Timothy syndrome. Nature 2011;471:230-234.

29 Leite LR, Henz BD, Macedo PG, Santos SN, Barreto JR, Zanatta A, Fenelon G, Cruz Filho FE: Catecholaminergic polymorphic ventricular tachycardia: a current overview. Future Cardiol 2009;5:191-199.

30 Liu N, Ruan Y, Priori SG: Catecholaminergic polymorphic ventricular tachycardia. Prog Cardiovasc Dis 2008;51:23-30.

31 Lahat H, Pras E, Olender T, Avidan N, Ben-Asher E, Man O, Levy-Nissenbaum E, Khoury A, Lorber A, Goldman B, Lancet D, Eldar M: A missense mutation in a highly conserved region of CASQ2 is associated with autosomal recessive catecholamine-induced polymorphic ventricular tachycardia in Bedouin families from Israel. Am J Hum Genet 2001;69:1378-1384.

32 Lehnart SE, Wehrens XH, Kushnir A, Marks AR: Cardiac ryanodine receptor function and regulation in heart disease. Ann N Y Acad Sci 2004;1015:144-159.

33 Jiang D, Xiao B, Zhang L, Chen SR: Enhanced basal activity of a cardiac Ca^{2+} release channel (ryanodine receptor) mutant associated with ventricular tachycardia and sudden death. Circ Res 2002;91:218-225.

34 Cerrone M, Colombi B, Santoro M, di Barletta MR, Scelsi M, Villani L, Napolitano C, Priori SG: Bidirectional Ventricular Tachycardia and Fibrillation Elicited in a Knock-In Mouse Model Carrier of a Mutation in the Cardiac Ryanodine Receptor. Circulation Research 2005;96:e77-e82.

35 Cerrone M, Napolitano C, Priori SG: Catecholaminergic polymorphic ventricular tachycardia: A paradigm to understand mechanisms of arrhythmias associated to impaired $Ca^{(2+)}$ regulation. Heart Rhythm 2009;6:1652-1659.

36 Wehrens XH: The molecular basis of catecholaminergic polymorphic ventricular tachycardia: what are the different hypotheses regarding mechanisms? Heart Rhythm 2007;4:794-797.

37 Esteban MA, Wang T, Qin B, Yang J, Qin D, Cai J, Li W, Weng Z, Chen J, Ni S, Chen K, Li Y, Liu X, Xu J, Zhang S, Li F, He W, Labuda K, Song Y, Peterbauer A, Wolbank S, Redl H, Zhong M, Cai D, Zeng L, Pei D: Vitamin C enhances the generation of mouse and human induced pluripotent stem cells. Cell Stem Cell 2010;6:71-79.

38 Yu J, Vodyanik MA, Smuga-Otto K, Antosiewicz-Bourget J, Frane JL, Tian S, Nie J, Jonsdottir GA, Ruotti V, Stewart R, Slukvin, II, Thomson JA: Induced pluripotent stem cell lines derived from human somatic cells. Science 2007;318:1917-1920.

39 Mummery C, Ward-van Oostwaard D, Doevendans P, Spijker R, van den Brink S, Hassink R, van der Heyden M, Opthof T, Pera M, de la Riviere AB, Passier R, Tertoolen L: Differentiation of human embryonic stem cells to cardiomyocytes: role of coculture with visceral endoderm-like cells. Circulation 2003;107:2733-2740.

40 Tost J, Dunker J, Gut IG: Analysis and quantification of multiple methylation variable positions in CpG islands by Pyrosequencing. Biotechniques 2003;35:152-156.

41 Caspersson T, Lomakka G, Zech L: The 24 fluorescence patterns of the human metaphase chromosomes - distinguishing characters and variability. Hereditas 1972;67:89-102.

42 Reppel M, Boettinger C, Hescheler J: Beta-adrenergic and muscarinic modulation of human embryonic stem cell-derived cardiomyocytes. Cell Physiol Biochem 2004;14:187-196.

43 Cleemann L, Morad M: Role of Ca^{2+} channel in cardiac excitation-contraction coupling in the rat: evidence from Ca^{2+} transients and contraction. J Physiol 1991;432:283-312.

44 Satin J, Itzhaki I, Rapoport S, Schroder EA, Izu L, Arbel G, Beyar R, Balke CW, Schiller J, Gepstein L: Calcium handling in human embryonic stem cell-derived cardiomyocytes. Stem Cells 2008;26:1961-1972.

45 Liu N, Colombi B, Memmi M, Zissimopoulos S, Rizzi N, Negri S, Imbriani M, Napolitano C, Lai FA, Priori SG: Arrhythmogenesis in Catecholaminergic Polymorphic Ventricular Tachycardia. Circulation Research 2006;99:292-298.

46 Nakajima T, Kaneko Y, Taniguchi Y, Hayashi K, Takizawa T, Suzuki T, Nagai R: The mechanism of catecholaminergic polymorphic ventricular tachycardia may be triggered activity due to delayed afterdepolarization. Eur Heart J 1997;18:530-531.

47 Paavola J, Viitasalo M, Laitinen-Forsblom PJ, Pasternack M, Swan H, Tikkanen I, Toivonen L, Kontula K, Laine M: Mutant ryanodine receptors in catecholaminergic polymorphic ventricular tachycardia generate delayed afterdepolarizations due to increased propensity to Ca^{2+} waves. Eur Heart J 2007;28:1135-1142.

48 Liu N, Colombi B, Memmi M, Zissimopoulos S, Rizzi N, Negri S, Imbriani M, Napolitano C, Lai FA, Priori SG: Arrhythmogenesis in catecholaminergic polymorphic ventricular tachycardia: insights from a RyR2 R4496C knock-in mouse model. Circ Res 2006;99:292-298.

49 Lehnart SE, Wehrens XH, Marks AR: Calstabin deficiency, ryanodine receptors, and sudden cardiac death. Biochem Biophys Res Commun 2004;322:1267-1279.

50 Marx SO, Reiken S, Hisamatsu Y, Jayaraman T, Burkhoff D, Rosemblit N, Marks AR: PKA phosphorylation dissociates FKBP12.6 from the calcium release channel (ryanodine receptor): defective regulation in failing hearts. Cell 2000;101:365-376.

51 Wehrens XH, Lehnart SE, Huang F, Vest JA, Reiken SR, Mohler PJ, Sun J, Guatimosim S, Song LS, Rosemblit N, D'Armiento JM, Napolitano C, Memmi M, Priori SG, Lederer WJ, Marks AR: FKBP12.6 deficiency and defective calcium release channel (ryanodine receptor) function linked to exercise-induced sudden cardiac death. Cell 2003;113:829-840.

52 Wehrens XH, Lehnart SE, Reiken SR, Deng SX, Vest JA, Cervantes D, Coromilas J, Landry DW, Marks AR: Protection from cardiac arrhythmia through ryanodine receptor-stabilizing protein calstabin2. Science 2004;304:292-296.

53 Blayney LM, Jones JL, Griffiths J, Lai FA: A mechanism of ryanodine receptor modulation by FKBP12/12.6, protein kinase A, and K201. Cardiovasc Res 2010;85:68-78.

54 Lehnart SE, Mongillo M, Bellinger A, Lindegger N, Chen BX, Hsueh W, Reiken S, Wronska A, Drew LJ, Ward CW, Lederer WJ, Kass RS, Morley G, Marks AR: Leaky Ca^{2+} release channel/ryanodine receptor 2 causes seizures and sudden cardiac death in mice. J Clin Invest 2008;118:2230-2245.

55 Kaufman ES: Mechanisms and clinical management of inherited channelopathies: long QT syndrome, Brugada syndrome, catecholaminergic polymorphic ventricular tachycardia, and short QT syndrome. Heart Rhythm 2009;6:S51-55.

56 Watanabe H, Knollmann BC: Mechanism underlying catecholaminergic polymorphic ventricular tachycardia and approaches to therapy. J Electrocardiol 2011;44:650-655.

57 Liu N, Denegri M, Ruan Y, Avelino-Cruz JE, Perissi A, Negri S, Napolitano C, Coetzee WA, Boyden PA, Priori SG: Short Communication: Flecainide Exerts an Antiarrhythmic Effect in a Mouse Model of Catecholaminergic Polymorphic Ventricular Tachycardia by Increasing the Threshold for Triggered Activity/Novelty and Significance. Circulation Research 2011;109:291-295.

58 Watanabe H, Chopra N, Laver D, Hwang HS, Davies SS, Roach DE, Duff HJ, Roden DM, Wilde AA, Knollmann BC: Flecainide prevents catecholaminergic polymorphic ventricular tachycardia in mice and humans. Nat Med 2009;15:380-383.

59 Kobayashi S, Yano M, Uchinoumi H, Suetomi T, Susa T, Ono M, Xu X, Tateishi H, Oda T, Okuda S, Doi M, Yamamoto T, Matsuzaki M: Dantrolene, a therapeutic agent for malignant hyperthermia, inhibits catecholaminergic polymorphic ventricular tachycardia in a RyR2(R2474S/+) knock-in mouse model. Circ J 2010;74:2579-2584.

60 Zhou Q, Xiao J, Jiang D, Wang R, Vembaiyan K, Wang A, Smith CD, Xie C, Chen W, Zhang J, Tian X, Jones PP, Zhong X, Guo A, Chen H, Zhang L, Zhu W, Yang D, Li X, Chen J, Gillis AM, Duff HJ, Cheng H, Feldman AM, Song LS, Fill M, Back TG, Chen SR: Carvedilol and its new analogs suppress arrhythmogenic store overload-induced $Ca^{(2+)}$ release. Nat Med 2011;17:1003-1009.

61 Davis RP, van den Berg CW, Casini S, Braam SR, Mummery CL: Pluripotent stem cell models of cardiac disease and their implication for drug discovery and development. Trends Mol Med 2011;17:475-484.

62 Wang Y, Mah N, Prigione A, Wolfrum K, Andrade-Navarro MA, Adjaye J: A transcriptional roadmap to the induction of pluripotency in somatic cells. Stem Cell Rev 2010;6:282-296.

63 Osafune K, Caron L, Borowiak M, Martinez RJ, Fitz-Gerald CS, Sato Y, Cowan CA, Chien KR, Melton DA: Marked differences in differentiation propensity among human embryonic stem cell lines. Nat Biotechnol 2008;26:313-315.

Fatima/Xu/Shao/Papadopoulos/Lehmann/Arnáiz-Cot/Rosa/Nguemo/
Matzkies/Dittmann/Stone/Linke/Zechner/Beyer/Hennies/Rosenkranz/
Klauke/Parwani/Haverkamp/Pfitzer/Farr/Cleemann/Morad/Milting/
Hescheler/Šarić